

A Novel Bilayer Propionyl-L-carnitine Loaded Polyvinyl Alcohol/Calcium Alginate/Carboxymethyl Cellulose wound dressing for the treatment of diabetic wounds: an in vitro and in vivo study

Wenjun Jiang

University of Electronic Science and Technology of China

Zuoyao Huang

University of Electronic Science and Technology of China

Weixiang Min

University of Electronic Science and Technology of China

Hao Zhang (✉ haozhang2021@gmail.com)

University of Electronic Science and Technology of China

Research Article

Keywords: Diabetic wounds, Wound dressing, Propionyl-L-carnitine, Carboxymethyl Cellulose, Polyvinyl Alcohol, Calcium Alginate

Posted Date: February 12th, 2021

DOI: <https://doi.org/10.21203/rs.3.rs-217915/v1>

License: © ⓘ This work is licensed under a Creative Commons Attribution 4.0 International License.

[Read Full License](#)

A Novel Bilayer Propionyl-L-carnitine Loaded Polyvinyl Alcohol/Calcium Alginate/Carboxymethyl Cellulose wound dressing for the treatment of diabetic wounds: an in vitro and in vivo study

Wenjun Jiang^{1,5,a}, Zuoyao Huang^{2,a}, Weixiang Min^{3,5,*}, Hao Zhang^{4,5,**}

1 Department of Pediatric Surgery, Sichuan Provincial People's Hospital, University of Electronic Science and Technology of China; Chengdu shichuan 610072 China

2 Department of Orthopaedics, Jinniu District People's Hospital of Chengdu; Chengdu Sichuan 610036, China

3 Department of anesthesiology, Sichuan Provincial People's Hospital, University of Electronic Science and Technology of China; Chengdu shichuan 610072, China

4 Department of Hepatobiliary Surgery, Sichuan Provincial People's Hospital, University of Electronic Science and Technology of China; Chengdu shichuan 610072, China

5 Chinese Academy of Sciences Sichuan Translational Medicine Research Hospital, Chengdu 610072, China

*Corresponding Author: Weixiang Min, E-mail: mmwxx2020@163.com

**co-corresponding author Hao Zhang, E-mail: hawerchina@gmail.com

a Wenjun Jiang and Zuoyao Huang contributed equally to this work.

Abstract

In the current study a drug delivering bilayer porous/nanofibrous wound dressing was developed using a combination of electrospinning and freeze-drying methods. The wound dressings were prepared by lyophilization of 1:1 weight ratios of calcium alginate and carboxymethyl cellulose (CMC) solutions. Drug delivering nanofibrous sheets were fabricated by electrospinning of polyvinyl alcohol (PVA) solution incorporated with 1%,3%,5%, and 10% of Propionyl-L-carnitine. The dressings were studied regarding their microstructure, swelling capacity, mechanical strength, surface wettability, water vapor permeability, drug release profile, in vitro degradation, cell viability assay, hemocompatibility, porosity measurement, microbial penetration assay, and protein adsorption assay. Based on in vitro studies, PVA sheets loaded with 5% Propionyl-L-carnitine was chosen for the preparation of wound dressings. The healing potential of the produced constructs was studied in rat model of diabetic wound. Our results showed that the drug delivering dressings demonstrated significantly higher wound closure and better histological regeneration compared to drug free constructs and sterile gauze. Our results suggest potential applicability of Propionyl-L-carnitine delivering Calcium Alginate/CMC/PVA dressing for the treatment of diabetic wounds in clinic.

Key words: Diabetic wounds; Wound dressing; Propionyl-L-carnitine; Carboxymethyl Cellulose; Polyvinyl Alcohol; Calcium Alginate

58 **Declarations**

59 **Funding**

60 The authors did not receive support from any organization for the submitted work.

61 **Conflicts of interest**

62 The authors have no conflicts of interest to declare that are relevant to the content of this article.

63 **Ethics approval**

64 The animal studies were approved by ethics committee of University of Electronic Science and Technology of China
65 and were performed in accordance with the university guidelines.

66

67

68

69

70

71

72

73

74

75

76

77

78

79

80

81

82

83

Introduction

Wounds are defined by integrity loss of skin tissue which can be caused by thermal, physical, or chemical injuries (Tarassoli et al. 2018). Given the fact that skin tissue has an inherent healing potential following injuries; in most cases, this tissue can repair its damages (Yu et al. 2019). However, in case of critical-sized defects or in disordered health conditions such as diabetes mellitus, wounds may turn into chronic non-healing wounds (Sahana and Rekha 2018). In diabetic patients, the angiogenesis and re-epithelialization processes are disturbed which hampers normal tissue repair responses. In addition, elevated inflammatory responses, poor blood flow, and oxidative damages result in a non-permissive environment for normal wound healing (Cho et al. 2019; Vijayakumar et al. 2019). In such patients, the application of a proper wound care product seems crucial. Among various marketed products, the use of biopolymer-based wound dressings has gained significant attention during the past decades (Shah et al. 2019). In this regard, alginate has been widely exploited in various forms such as hydrogel, films, nanofibrous yarns, and composites to produce wound care material (Akbar et al. 2018; Jeong et al. 2020). Therapeutic appeal towards this polymer stems from its biocompatibility, biodegradability, non-immunogenicity, its high capacity to absorb wound exudates, and low cost (Aderibigbe and Buyana 2018). To further enhance the alginate's capacity to heal wounds; in the current research, Carboxymethyl cellulose (CMC) was blended with alginate to produce wound dressings. CMC can maintain a moist environment for wound healing and can absorb large amounts of wound exudates which is particularly favorable in treating diabetic wounds (Li et al. 2016; Trevisol et al. 2019). Despite showing promising results in previous studies, the proposed wound dressing lacks enough bioactivity for a successful wound healing. Therefore, in this study we hypothesized using an electrospun Propionyl-L-carnitine-loaded Polyvinyl Alcohol (PVA) nanofibrous sheet as a drug delivery system to develop the wound care material. This drug is required for fatty acids metabolism in mitochondria. In addition, it has been shown that Propionyl-L-carnitine is an anti-oxidant agent which can protect cells from oxidative damages and can increase blood flow in ischemic tissues (Scioli et al. 2015). PVA is a hydrophilic biomaterial which its unique properties have made it an ideal carrier for hydrophilic drugs (Li et al. 2013; Orienti et al. 2001). Electrospinning is a versatile and affordable method for scaffold fabrication. The prepared constructs have nanofibrous structures which have a strong resemblance to Extracellular Matrix architecture. Furthermore, the produced nanofibers have a relatively large surface area and can be exploited as a programmable drug delivery platform (Sill and Von Recum 2008). The aim of the current study is to evaluate the healing potential of a bilayer Calcium alginate/CMC/Propionyl-L-carnitine loaded PVA scaffolds in a rat model of diabetic wound.

Methods and materials

Chemicals

The materials and solvents were purchased from Sigma-Aldrich (St. Louis, USA) and Merck (Darmstadt, Germany), respectively, unless otherwise noted.

Fabrication of Calcium alginate/CMC films

Firstly, sodium alginate of medium-viscosity (61% of mannuronic and 39% of guluronic acid) and CMC of medium viscosity (degree of substitution 0.7) were dissolved separately in glycerol containing distilled water (glycerol: polymer weight ratio was 60%) at final concentration of 1.5% (wt%) and stirred for 24 hours at room temperature. Then, Calcium chloride at final concentration 2% (wt%) in distilled water was added to the alginate solution at volume ratio of 1:4 to begin the cross linking process and stirred for further 24 h at room temperature. The equal amounts of each solution were blended to obtain a 1;1 alginate/CMC solution and stirred for 24 h. The prepared mixture was transferred into -20 ° C and incubated for 24 h. The solidified sample was then kept at -80 °C for further 24 h. Then, the samples were freeze-dried (Telstar, Terrassa, Spain) for 48 h.

Fabrication of Propionyl-L-carnitine loaded PVA scaffolds

Firstly, PVA (Mw = 72 kDa) at final concentration of 12% was dissolved in distilled water for 24 h at room temperature. Then, Propionyl-L-carnitine (at weight ratios of 1%, 3%,5%, and 10% was added to the PVA solution and thoroughly mixed for 8h. The prepared solution was transferred to a 10 ml syringe connecting to an 18-gauge metal needle. The samples then fixed in the peristaltic pump of electrospinning device (Santa Marta co ltd, USA). The electrospinning began by applying a positive high voltage of 16 to 18 kv. The needle to mandrel distance set at 15 cm and the polymer feeding rate was 1 ml/h. The electrospinning continued until the mandrel was fully covered by the nanofibers. The prepared sheets were cross-linked according to a method described previously (Stone et al. 2013).

Scanning electron microscopy imaging of the samples

To analyze the microstructure of the constructs, they were imaged under and SEM device (AIS2100, Seron Technology, South Korea) at an accelerating voltage of 20 kV, after the sputter coating with gold for 250 s using a sputter coater (SC7620, Quorum Technologies, England).

Swelling studies on Calcium alginate/CMC films

The swelling properties of the Calcium alginate/CMC films was studied using a method as described previously (Ehterami et al. 2019). Briefly, the freeze-dried samples were immersed in 10 ml of phosphate buffer solution (PBS) and incubated for 3 days. After predetermined time points, the samples were taken out and immediately weighed. The swelling ratio of the samples was calculated according to the following equation.

$$\text{Swelling ratio: } \frac{m1-m0}{m0} \times 100$$

Where m1 is the swollen weight of samples and m0 is the dry weight of the films.

Mechanical strength measurement

The mechanical properties of the scaffolds were studied using a uniaxial tensile testing device (Softon Technologies, USA) at an extension rate of 1 mm/min,

Contact angle measurement

149 The surface hydrophilicity of the samples was studied using a static contact angle measuring device (KRUSS,
150 Hamburg, Germany). A water droplet was placed on different spots of each scaffold and the angle between its surface
151 and the scaffolds was calculated and averaged.

152 **Water vapor permeability study**

153 To assess the dressing's capability for gas transfer, this experiment was performed on scaffolds. 10 ml of distilled
154 water was poured into an empty bottle and then capped by the fabricated dressings and then incubated at 33 °C for 12
155 hours, the evaporated water through the scaffolds was calculated using the following equation.

156 Water vapor permeability = $\frac{W}{AT}$

157 Where w is mass of evaporated water, A is surface area, and T is the time of incubation.

158 **In vitro degradation profile of the samples**

159 The degradation rate of the scaffolds was studied by immersing predetermined amounts of each scaffold in 10 ml of
160 PBS solution at 37 °c under gentle shaking over a period of 10 days. After each time point, the samples were taken
161 out, dried, and weighed. Weight loss was measured according to the following equation.

162 Weight loss = $\frac{w_0 - w_1}{w_0} \times 100$

163 where W0 is the initial weight of the films and W1 is the dry weight

164 after removal from the PBS solution.

165 **Porosity assessment**

166 The porosity of the scaffolds was studied using liquid displacement method. The samples were immersed in known
167 volume of ethanol and incubated for 1 hour. After this time period, samples were taken out and the residual ethanol
168 volume was recorded. The porosity of the scaffolds was calculated using the following equation.

169 Porosity (%) = $\frac{v_1 - v_3}{v_2 - v_3} \times 100$

170 Where v1 is the initial volume of ethanol, v2 is the volume of ethanol after scaffolds immersion, and v3 is the volume
171 of ethanol after scaffold's removal.

172 **Release profile of Propionyl-L-carnitine from PVA films**

173 To evaluate the release profile of Propionyl-L-carnitine from PVA films, high-performance liquid chromatography
174 method was exploited as described previously (Marzo et al. 1988). Briefly, the drug loaded PVA fibers were immersed
175 in PBS solution for 24 h at 37 °c under gentle shaking. At different time intervals, 1 ml of the samples was obtained
176 and replaced with fresh PBS solution. The harvested medium was used to measure cumulative release profile of
177 Propionyl-L-carnitine from PVA fibers.

178

179

180 **Microbial penetration assay**

181 In each group, 10 ml bottles filled with 5 ml of BHI broth culture medium was covered by the prepared constructs and
182 incubated at room temperature. The invasion of the bacteria into the growth medium was studied at 3 and 7 days' time
183 points. Vials capped with the sterile gauze and open vials were used as negative and positive controls, respectively.
184 The blurred growth mediums as the indication of bacterial growth was analyzed using a spectroscopy method at 600
185 nm using a microplate spectrophotometer.

186 **Protein adsorption assay**

187 To evaluate the ability of the constructs to adsorb protein they were studied via batch contact method as described
188 previously (Golafshan et al. 2017). Briefly, films with known weigh were immersed in PBS for 4 h and then weighed.
189 Then, the swollen samples were immersed in 20 ml of 0.2 wt% of Bovine Serum Albumin (BSA) solution and
190 incubated at 37 °C for 30 minutes under gentle shaking. The samples were taken out and the residual proteins in the
191 supernatant was determined by spectrophotometric method at 280 nm. The amount of adsorbed protein on the film's
192 surface was calculated using the following equation:

193 Adsorbed protein (mg) = $\frac{C1-C0}{w} \times V$

194 Where c1 is the initial protein concentration of BSA, C0 is the protein concentration after scaffolds soaking and
195 removal, w is the weight of swollen scaffold, and V is the volume of BSA.

196 **Blood compatibility assay.**

197 8ml of whole blood was obtained from a healthy volunteer and mixed with 1 ml of 3.8% Sodium citrate anticoagulant.
198 This sample was diluted with 2.5 ml normal saline solution. 200 µl of this blood was poured onto the samples and
199 incubated at 37 °C for 60 min. Then, the scaffolds were taken out and the residual blood was centrifuged at 1500 rpm
200 for 10 min. The absorbance value of the samples was read at 545 nm using a Multi-Mode Microplate Reader. The
201 blood samples diluted with normal saline and distilled water was used as positive control and negative control
202 respectively. The percentage of hemolysis was calculated using the following equation.

203 Percentage of hemolysis (%): $\frac{Dt-Dnc}{Dpc-Dnc} \times 100$

204 Where Dt is the absorbance values of the studied group, Dnc and Dpc is the absorbance for negative control and
205 positive control respectively.

206 **Cell viability assay**

207 The MTT (3-(4, 5-dimethylthiazol-2-yl)-2, 5 diphenyl tetrazolium bromide, GIBCO-BRL, Eggenstein, Germany) test
208 was exploited to study the proliferation rate of L-929 cells cultured on the constructs. Cells were seeded on drug

loaded PVA sheets and Calcium alginate/CMC films at a density of 1×10^4 cells per sample and cultured for 7 days in Dulbecco's modified Eagle's medium: nutrient mixture F-12 supplemented with 10% (v/v) fetal bovine serum, 100 unit/ml of penicillin (Sigma-Aldrich, USA) and 100 $\mu\text{g}/\text{ml}$ of streptomycin (Sigma-Aldrich, USA) in a humidified incubator at 37°C with 5% CO_2 . At each time point, the media on the samples was removed and replaced with 200 μl of .5 mg/ml MTT solution and incubated for 4 h at a dark condition. After this time period, the MTT solution was discarded and replaced with 100 μl DMSO solution to dissolve any formed formazan crystals. The absorption values were recorded at 570 nm.

Animal studies

The animal studies were approved by ethics committee of University of Electronic Science and Technology of China and were performed in accordance with the university guidelines. Diabetes mellitus was induced in adult male Wistar rats. Briefly, a single dose of 55 mg/kg STZ in citrate buffer (pH 4.4, 0.1 M) was administered into intraperitoneal soft tissue and rats administered with citrate buffer served as control group. Blood samples were obtained from retro-orbital plexus veins and the blood glucose level was measured. The rats whose serum glucose level was more than 250 mg/dl met the criteria for diabetes mellitus otherwise they were excluded from the study. For the creation of in vivo wound healing model, the rats were anesthetized by intraperitoneal injection of Ketamine 5%/Xylazine 2% (70 mg ketamine and 6 mg Xylazine/1 kg body weight). The rats' back was shaved and disinfected using povidone iodine and a $1.5 \times 1.5 \text{ cm}^2$ of their skin was excised (Fig. 1). The rats were divided into 3 groups (5 animals per group) namely group A in which wounds were covered with Calcium alginate/CMC/ Propionyl-L-carnitine-loaded PVA scaffolds, group B in which the rats were treated with Calcium alginate/CMC/ Drug free PVA scaffolds, and negative control in which sterile gauze was used to cover the wounds. For wound dressing's application, PVA films were placed directly on the wound tissue then Calcium alginate/CMC films covered the PVA sheets. The whole bilayer wound dressing was fixed in place by using an elastic adhesive bandage. The wound dressings were changed on daily basis. To evaluate the wound size reduction, the macroscopic appearance of the wounds was imaged at day 7 and 14 using a digital camera (Canon Inc., Tokyo, Japan). The percentage of wound contraction was calculated using the following equation:

$$\text{Percentage of wound closure} = \left(1 - \frac{\text{open wound area}}{\text{initial wound area}} \right) \times 100$$

After 14 days of post-wounding, the animals were humanely killed by ketamine overdose and the wound tissues were harvested for histopathological examinations. After processing and embedding in paraffin the samples were sectioned and underwent tissue staining with hematoxylin-eosin (H&E) and Masson's trichrome (MT). To prevent bias, an independent pathologist reported the pathological changes under a light microscope (Carl Zeiss, Thornwood, USA) with a digital camera (Olympus, Tokyo, Japan). Epithelial tissue thickness, recruitment of macrophages, fibroplasia,

and new blood vessel formation were studied. Furthermore, collagen deposition was also measured according to histopathological images.

Results

Microstructure studies

The microstructure of the scaffolds was observed using scanning electron microscopy imaging. The results (Fig. 2 a) showed the Calcium alginate/CMC films had porous structure with interconnectivity of the pores. The pore size measurement using Image J software (National Institutes of Health, Bethesda, USA) showed that the average pore size was around 50 -100 μm . This porous structure of the membranes can facilitate gas exchanges and prevent wound maceration. This would inhibit establishing a non-aerobic condition for bacterial growth. In addition, this porous structure would also facilitate wound exudates absorption (Karahaliloglu et al. 2017; Komatsuzaki et al. 1994). Fig. 2 b shows microstructure for PVA scaffolds loaded with 5% Propionyl-L-carnitine. As shown, the nanofibers had randomly oriented structure with smooth morphology. Twenty points of images were selected for fiber size measurement and the results showed that the fibers had 1136.03 ± 52.67 nm diameter. Structural resemblance of the produced scaffolds to native extracellular matrix architecture is particularly favorable for stimulating fibroblasts' migration, attachment, and proteins production which will have a profound effect in wound closure (Chen et al. 2008; Gu et al. 2009).

Swelling studies of Calcium alginate/CMC films

Swelling study of the membranes was conducted to test their ability to form hydrogel and marinating a moist environment upon exudates absorption. Non-cross linked alginate polymer will turn into sol when it absorbs water while when cross linked with calcium ion it will be able to form hydrogel upon water absorption (Novikova et al. 2006). Fig. 3 illustrates time course swelling of Calcium alginate/CMC membranes in 72 h time period. As shown, the percentage of swelling reaches to the highest level of 362.33 ± 15.29 % after 4 h of scaffold immersion and then decreases to the 111.66 ± 8.97 % at 72 h. As the dressings are changed on daily basis therefore they can absorb the wound exudates to their utmost capacity within few hours of dressing's application.

Cumulative release profile of Propionyl-L-carnitine from PVA nanofibers

The ability of the bioactive dressing to sustain release the loaded drug in the wound bed is of paramount importance. As shown in Fig. 4, the cumulative release of Propionyl-L-carnitine from PVA films could reach to 80.06 ± 4.38 % after 24 h of incubation. Therefore, the designed delivery system will be able to deliver almost all the loaded drug to the wound bed in a sustained manner. The drug release from polymeric matrices has a direct relation with the degradation rate. Given the fact that PVA is a fast-degrading polymer; even after cross linking, this polymer is particularly interesting in developing drug delivering wound dressings since they are usually replaced on daily basis (Hamad et al. 2014).

Degradation rate measurement

The in vitro degradation study showed that the percentage of weight loss for Calcium alginate/CMC scaffolds could reach to 44.39 ± 3.37 % and 55.72 ± 69 % after 5 days and 10 days respectively. While, PVA sheets almost fully degraded within 24 h of incubation in PBS solution.

Porosity measurement

Porosity evaluation showed that the Calcium alginate/CMC scaffolds had 83.57 ± 4.38 % which is ideal for a tissue engineered construct (Salehi et al. 2018).

Blood compatibility test

Results of hemolysis assay of different samples are shown in Fig. 5. The study revealed that the Calcium alginate/CMC membrane had significantly higher OD values compared to PVA sheets and negative control groups. This could be due to hemostatic effects of calcium alginate which is in accordance with previous studies. Calcium Alginate can promote blood coagulation and cause hemostasis which is the first phase of wound healing (TAŞKIN et al. 2013). Positive control had significantly higher absorbance values compared to other groups.

Cell viability assay

To study the metabolic activity and proliferation rate of L929 cells on different scaffolds, MTT assay was conducted at days 1, 3, and 7. As shown in Fig. 6 a, there was no significant deference between Calcium alginate/CMC films and control group at different time intervals, implying that the prepared construct was not toxic against L929 cells. In drug-loaded PVA groups (Fig. 6 b), at day 1 PVA fibers incorporated with 5% Propionyl-L-carnitine had significantly higher absorbance values compared to other groups. This trend was almost unchanged towards the day 7. According to this assay, we assumed that 5% of Propionyl-L-carnitine was optimal concentration which had a beneficial effect on fibroblasts' metabolic activity. Therefore, this concentration was chosen for treating skin wounds.

Microbial penetration assay

An ideal wound care product should prevent microbial invasion into the wound bed (Samadian et al. 2020). Our results showed that (Fig. 7) the bilayer wound dressing could significantly reduce bacterial colony formation in the growth medium. This can be due to physical barrier that PVA nanofibers may have caused. In addition, Wong et al. used CMC films for controlling bacterial wound infection. Infected wounds were treated with CMC films and it was revealed that the membranes could attach to the bacteria and remove them from the wound tissue (Wong and Ramli 2014). Therefore, it is hypothesized that the CMC polymer in the bilayer wound dressing attached to the bacteria and prevented them from invading the growth medium.

Water vapor permeability study

Interestingly; in our fabrication method, the water vapor transmission capability of the dressings can be tailored to obtain the optimal moist environment for wound healing. This can be achieved through tailoring the polymer concentrations, altering the freeze-drying parameters, or using filler materials. Our study showed that the bilayer wound dressing had 11.98 ± 1.37 mg/cm²/h of water vapor permeation.

Contact angle measurement

Generally, hydrophobic materials are not suitable for wound dressing applications since they lack enough capacity for water absorption (Jin et al. 2016). Therefore, surface contact angle measurement was performed to evaluate the dressings surface wettability. The results showed that the PVA/5% Propionyl-L-carnitine had 64.39 ± 4.28 ° and Calcium alginate/CMC films had 56.19 ± 2.15 ° of contact angle.

Tensile strength measurement

An acceptable mechanical strength is essential for wound dressing handling during the dressing's application. Our study revealed that the prepared constructs' mechanical properties were in acceptable range which is from 0.7 to 18 Mpa (Samadian et al. 2020). The PVA/5% Propionyl-L-carnitine sheets had $2.68 \pm .24$ Mpa tensile strength and Calcium alginate/CMC films had $3.53 \pm .67$ Mpa tensile strength.

Protein adsorption assay

At the initial phases of thrombosis on a biomaterial surface, proteins are adsorbed and initiate a series of events which eventually cause thrombosis. Therefore, better protein adsorption properties are pro-thrombotic for a wound dressing (Golafshan et al. 2017). Our data showed that the amount of adsorbed protein to PVA/5% Propionyl-L-carnitine sheets was around $3.25 \pm .49$ mg while the Calcium alginate/CMC films could adsorb $5.84 \pm .35$ mg to its surface. When a biomaterial is exposed to biological fluids its surface gets hydrated and a thin layer is formed which leads to adsorption of series of different proteins. This phenomenon depends on the surface chemistry and the higher the hydrophilicity, the lower the protein adsorption. Since by increasing the surface wettability the energetic cost for surface dehydration also increases hence lowering the protein replacement at the surface (Vogler 2012).

In vivo wound healing

The healing potential of the bilayer wound dressing was investigated in a rat model of diabetic wound. Fig. 8 shows the percentage of wound closure for wounds treated with different materials. As shown, the rats treated with drug loaded wound dressing had significantly higher wound closure compared to drug free composites and negative control groups. The percentage of wound contraction for drug loaded wound dressing could reach to 67.39 ± 5.26 % and 92.49 ± 6.19 % at 7 days and 14 days post-wounding respectively. While, this value for drug free membranes was 56.49 ± 3.38 % and 79.67 ± 4.29 % at day 7 and 14 of surgery respectively. Histopathological examinations evaluated the healing potential of different groups and the results are shown in Figure 9. In the negative control group, the presence of inflammatory cells and disintegrated collagen depositions was evident. In addition, epidermal layer is not formed in this group. In Calcium alginate/CMC/PVA 5% Propionyl-L-carnitine group, epithelialization had been completed and less inflammatory cells were observed. Moreover, skin appendices regeneration was observed in this

group as evidenced by the presence of normal rete ridges, sebaceous glands, and hair follicles. Overall structure of the repaired skin in this group had more resemblance to positive control group. The histomorphometric study revealed that the epithelial thickness (Fig. 8 b) in drug delivering wound dressing was significantly higher compared to other groups. The epithelial thickness for Calcium alginate/CMC/PVA 5% Propionyl-L-carnitine group was 48.13 ± 5.49 μm . While, Calcium alginate/CMC/PVA and negative control groups exhibited the epithelial thickness of 31.52 ± 6.87 μm and 6.19 ± 1.61 μm respectively. Wound tissue in the negative control group had immature granulation tissue which was evidenced by ineffective wound closure. The wound contraction heavily depends on deposition of collagen molecules. Study revealed that the percentage of collagen deposition (Fig. 8 c) in Calcium alginate/CMC/PVA 5% Propionyl-L-carnitine group was significantly greater than Calcium alginate/CMC/PVA group (78.31 ± 7.26 % vs. 64.59 ± 6.01 %, p value < 0.05).

Discussion

The main goal of skin tissue engineering is to develop products which results in prompt aesthetic and functional recovery of skin with negligible scarring (Mansbridge 2008). In this way, tissue engineered wound dressings need to have versatile properties to successfully support tissue repair and manage different phases of wound healing (Chen et al. 2009). Wound healing is a complex process which is composed of different interrelated phases known as hemostasis, inflammatory phase, proliferation phase, and remodeling phase (George Broughton et al. 2006). In every step of wound healing, specific biomaterials and signaling molecules can be used to drive the healing process. In this regard, a variety of multi-potential wound dressings have been tested in previous studies (Boateng et al. 2008). For designing such dressings, material selection and optimization is the key step. Among different types of biomaterials, we exploited combined use Calcium alginate, CMC, and PVA to fabricate a drug delivering bilayer membrane. Alginate is a natural biomaterial that is harvested from brown seaweed. Its low cost, biocompatibility and non-toxicity has added to its therapeutic appeal for wound management applications (Aderibigbe and Buyana 2018). Dressings produced from this polymer maintain a moist environment conducive to fibroblasts and keratinocytes proliferation, migration, and functions (Zhang and Zhao 2020). CMC is another polysaccharide which can be exploited to promote wound healing. It can absorb huge amounts of wound exudates and can impart antibacterial properties to the fabricated dressing. In addition, dressings produced from this polymer can promote angiogenesis and autolytic debridement (Kanikireddy et al. 2020). To facilitate fast release of Propionyl-L-carnitine into the wound bed we chose PVA for our drug delivery matrix. Our results showed that sheets produced from PVA could successfully release its drug cargo within 24 h. For fabrication of the dressings, we used a combination of freeze-drying and electrospinning methods. Lyophilization results in a porous structure which facilitates gas exchange and exudate absorption (Gonzaga et al. 2020). While, the electrospinning method produces scaffolds with structural resemblance to native extracellular matrix. In addition, the fabricated fibers have a high surface to volume ratio which makes them ideal carriers for a variety of drugs (Khalf and Madihally 2017). Although the proposed biomaterials have unique properties for wound healing, they lack enough bioactivity. To impart this property to the dressings, Propionyl-L-carnitine was incorporated into PVA nanofibers using electrospinning method. This substance is an ester of L-carnitine which is essential in fatty

acids metabolism. Furthermore, it has been shown that Propionyl-L-carnitine is an antioxidant agent and can prevent lipid peroxidation in elevated levels of reactive oxygen species (Di Emidio et al. 2020).

The healing potential of Propionyl-L-carnitine loaded bilayer wound dressing was evaluated in rat model of diabetic wound. The results showed that the drug delivering dressing group had significantly higher wound size reduction, epithelial thickness, and collagen deposition. Diabetic wounds are often accompanied by endothelial dysfunction and impaired blood flow (Kolluru et al. 2012). Pola et al. showed that Propionyl-L-carnitine can dramatically reduce wound size in patients with venous leg ulcer which was accompanied by enhanced blood flow in the patients (Pola et al. 1991). In addition, Stasi et al. showed that Propionyl-L-carnitine can improve blood flow and vascular function in a rabbit model of hind limb ischemia. They showed that Propionyl-L-carnitine had increased vasodilation through increasing nitric oxide (NO) plasma levels hence causing vasodilation in ischemic sites and formation of new blood vessels (Stasi et al. 2010). Scioli et al. reported that Propionyl-L-carnitine oral administration could improve skin flap viability. They could show that upregulation of inducible nitric oxide synthase (iNOS), vascular endothelial growth factor (VEGF), placental growth factor (PIGF) and reduction of NADPH-oxidase 4 (Nox4) expression. Endothelial dysfunction which is the major cause of diabetic wounds can be prevented through Nox4 inhibition (Scioli et al. 2015). Therefore, we assume that part of the observed healing effect could be due to inhibiting endothelial dysfunction and increasing blood flow in the wound site. Elevated levels of Reactive Oxygen Species (ROS) are associated with delayed wound healing in diabetic patients (Nouvong et al. 2016). Previous studies suggest the application of radical scavengers to modulate ROS levels in treating diabetic wounds (Naseri-Nosar et al. 2017). Vanella et al. showed that Propionyl-L-carnitine has radical scavenger, anti-oxidant, and DNA protective effects (Vanella et al. 2000). Furthermore, Gomez-amorez proved anti-oxidant activities of Propionyl-L-carnitine in liver and heart of spontaneously hypertensive rats (Gómez-Amores et al. 2006). Therefore, the anti-oxidant potential of this drug may also have contributed in the observed healing effects. However, more extensive researches at gene and protein levels need to be performed to further elucidate the underlying mechanisms of Propionyl-L-carnitine's contribution in treating diabetic wounds.

Conclusion

In summary, a bilayer drug loaded porous/nanofibrous polymeric wound dressing was fabricated in this study for the management of diabetic wounds. Our results revealed that scaffolds loaded with 5% Propionyl-L-carnitine exhibited the highest cell proliferation with fibroblasts. In vivo studies showed that the drug loaded wound dressing had significantly higher healing potential compared to drug free dressings and negative control. This preliminary study suggests potential applicability of this dressing to treat diabetic wounds in clinic.

Conflicts of interest

The authors declare no conflicts of interest with regard to this study.

410 **References**

- 411 Aderibigbe BA, Buyana B (2018) Alginate in wound dressings *Pharmaceutics* 10:42
- 412 Akbar MU, Zia KM, Akash MSH, Nazir A, Zuber M, Ibrahim M (2018) In-vivo anti-diabetic and wound
413 healing potential of chitosan/alginate/maltodextrin/pluronic-based mixed polymeric micelles:
414 Curcumin therapeutic potential *INT J BIOL MACROMOL* 120:2418-2430
- 415 Boateng JS, Matthews KH, Stevens HN, Eccleston GM (2008) Wound healing dressings and drug delivery
416 systems: a review *J PHARM SCI* 97:2892-2923
- 417 Chen J-P, Chang G-Y, Chen J-K (2008) Electrospun collagen/chitosan nanofibrous membrane as wound
418 dressing *COLLOID SURFACE A* 313:183-188
- 419 Chen M, Przyborowski M, Berthiaume F (2009) Stem cells for skin tissue engineering and wound healing
420 *CRIT REV BIOMED ENG* 37
- 421 Cho H, Blatchley MR, Duh EJ, Gerecht S (2019) Acellular and cellular approaches to improve diabetic
422 wound healing *ADV DRUG DELIVER REV* 146:267-288
- 423 Di Emidio G et al. (2020) Regulatory Functions of L-Carnitine, Acetyl, and Propionyl L-Carnitine in a PCOS
424 Mouse Model: Focus on Antioxidant/Antiglycative Molecular Pathways in the Ovarian
425 Microenvironment *Antioxidants* 9:867
- 426 Ehterami A et al. (2019) Chitosan/alginate hydrogels containing Alpha-tocopherol for wound healing in
427 rat model *J DRUG DELIV SCI TEC* 51:204-213
- 428 George Broughton I, Janis JE, Attinger CE (2006) Wound healing: an overview *PLAST RECONSTR SURG*
429 117:1e-S-32e-S
- 430 Golafshan N, RezaHasani R, Esfahani MT, Kharaziha M, Khorasani S (2017) Nanohybrid hydrogels of
431 laponite: PVA-Alginate as a potential wound healing material *CARBOHYD POLYM* 176:392-401
- 432 Gómez-Amores L, Mate A, Revilla E, Santa-María C, Vázquez CM (2006) Antioxidant activity of propionyl-
433 L-carnitine in liver and heart of spontaneously hypertensive rats *LIFE SCI* 78:1945-1952
- 434 Gonzaga Vda et al. (2020) Chitosan-laponite nanocomposite scaffolds for wound dressing application *J*
435 *BIOMED MATER RES B* 108:1388-1397
- 436 Gu S-Y, Wang Z-M, Ren J, Zhang C-Y (2009) Electrospinning of gelatin and gelatin/poly (l-lactide) blend and
437 its characteristics for wound dressing *MAT SCI ENG C* 29:1822-1828
- 438 Hamad D, Mehrvar M, Dhib R (2014) Experimental study of polyvinyl alcohol degradation in aqueous
439 solution by UV/H₂O₂ process *POLYM DEGRAD STABIL* 103:75-82
- 440 Jeong S, Kim B, Park M, Ban E, Lee S-H, Kim A (2020) Improved Diabetic Wound Healing by EGF
441 Encapsulation in Gelatin-Alginate Coacervates *Pharmaceutics* 12:334
- 442 Jin SG et al. (2016) Influence of hydrophilic polymers on functional properties and wound healing efficacy
443 of hydrocolloid based wound dressings *INT J PHARMACEUT* 501:160-166
- 444 Kanikireddy V, Varaprasad K, Jayaramudu T, Karthikeyan C, Sadiku R (2020) Carboxymethyl cellulose-
445 based materials for infection control and wound healing: A review *INT J BIOL MACROMOL*

446 Karahaliloglu Z, Kilicay E, Denkbaz EB (2017) Antibacterial chitosan/silk sericin 3D porous scaffolds as a
447 wound dressing material ARTIF CELL NANOMED B 45:1172-1185

448 Khalf A, Madihally SV (2017) Recent advances in multiaxial electrospinning for drug delivery EUR J PHARM
449 BIOPHARM 112:1-17

450 Kolluru GK, Bir SC, Kevil CG (2012) Endothelial dysfunction and diabetes: effects on angiogenesis, vascular
451 remodeling, and wound healing INT VASC MED 2012

452 Komatsuzaki S, Hirayama T, Toyokawa T (1994) Wound dressing having a porous structure. Google
453 Patents,

454 Li D, Ye Y, Li D, Li X, Mu C (2016) Biological properties of dialdehyde carboxymethyl cellulose crosslinked
455 gelatin-PEG composite hydrogel fibers for wound dressings CARBOHYD POLYM 137:508-514

456 Li X, Kanjwal MA, Lin L, Chronakis IS (2013) Electrospun polyvinyl-alcohol nanofibers as oral fast-dissolving
457 delivery system of caffeine and riboflavin COLLOID SURFACE B 103:182-188

458 Mansbridge J (2008) Skin tissue engineering J BIOMAT SCI-POLYM E 19:955-968

459 Marzo A, Monti N, Ripamonti M, Martelli EA (1988) Application of high-performance liquid
460 chromatography to the analysis of propionyl-L-carnitine by a stereospecific enzyme assay J
461 CHROMATOGR A 459:313-317

462 Naseri-Nosar M, Farzamfar S, Sahrapeyma H, Ghorbani S, Bastami F, Vaez A, Salehi M (2017) Cerium oxide
463 nanoparticle-containing poly (ϵ -caprolactone)/gelatin electrospun film as a potential wound
464 dressing material: in vitro and in vivo evaluation MATER SCI ENG C 81:366-372

465 Nouvong A, Ambrus AM, Zhang ER, Hultman L, Collier HA (2016) Reactive oxygen species and bacterial
466 biofilms in diabetic wound healing PHYSIOL GENOMICS

467 Novikova LN, Mosahebi A, Wiberg M, Terenghi G, Kellerth JO, Novikov LN (2006) Alginate hydrogel and
468 matrigel as potential cell carriers for neurotransplantation J BIOMED MATER RES A 77:242-252

469 Orienti I, Trere R, Zecchi V (2001) Hydrogels formed by cross-linked polyvinylalcohol as colon-specific drug
470 delivery systems DRUG DEV IND PHARM 27:877-884

471 Pola P, Flore R, Serricchio M, Tondi P (1991) New carnitine derivatives for the therapy of cutaneous ulcers
472 in vasculopathics DRUG EXP CLIN RES 17:277-282

473 Sahana T, Rekha P (2018) Biopolymers: Applications in wound healing and skin tissue engineering MOL
474 BIOL REP 45:2857-2867

475 Salehi M et al. (2018) Sciatic nerve regeneration by transplantation of Schwann cells via erythropoietin
476 controlled-releasing polylactic acid/multiwalled carbon nanotubes/gelatin nanofibrils neural
477 guidance conduit J BIOMED MATER RES B 106:1463-1476

478 Samadian H et al. (2020) Electrospun cellulose acetate/gelatin nanofibrous wound dressing containing
479 berberine for diabetic foot ulcer healing: in vitro and in vivo studies SCI REP 10

480 Scioli MG, Giudice PL, Bielli A, Tarallo V, De Rosa A, De Falco S, Orlandi A (2015) Propionyl-L-carnitine
481 enhances wound healing and counteracts microvascular endothelial cell dysfunction PLoS One
482 10:e0140697

483 Shah SA et al. (2019) Biopolymer-based biomaterials for accelerated diabetic wound healing: A critical
484 review INT J BIOL MACROMOL 139:975-993

485 Sill TJ, Von Recum HA (2008) Electrospinning: applications in drug delivery and tissue engineering
486 Biomaterials 29:1989-2006

487 Stasi MA et al. (2010) Propionyl-L-carnitine improves postischemic blood flow recovery and arteriogenic
488 revascularization and reduces endothelial NADPH-oxidase 4-mediated superoxide production
489 ARTERIOSCL THROM VAS 30:426-435

490 Stone SA, Gosavi P, Athauda TJ, Ozer RR (2013) In situ citric acid crosslinking of alginate/polyvinyl alcohol
491 electrospun nanofibers MATER LETT 112:32-35

492 Tarassoli SP, Jessop ZM, Al-Sabah A, Gao N, Whitaker S, Doak S, Whitaker IS (2018) Skin tissue engineering
493 using 3D bioprinting: an evolving research field J PLAST RECONSTR AES 71:615-623

494 TAŞKIN AK et al. (2013) The hemostatic effect of calcium alginate in experimental splenic injury model
495 Ulus Travma Acil Cerrahi Derg 19:195-199

496 Trevisol T, Fritz A, de Souza S, Bierhalz A, Valle J (2019) Alginate and carboxymethyl cellulose in monolayer
497 and bilayer films as wound dressings: Effect of the polymer ratio J APPL POLYM SCI 136:46941

498 Vanella A, Russo A, Acquaviva R, Campisi A, Di Giacomo C, Sorrenti V, Barcellona M (2000) L-propionyl-
499 carnitine as superoxide scavenger, antioxidant, and DNA cleavage protector CELL BIOL TOXICOL
500 16:99-104

501 Vijayakumar V, Samal SK, Mohanty S, Nayak SK (2019) Recent advancements in biopolymer and metal
502 nanoparticle-based materials in diabetic wound healing management INT J BIOL MACROMOL
503 122:137-148

504 Vogler EA (2012) Protein adsorption in three dimensions Biomaterials 33:1201-1237

505 Wong TW, Ramli NA (2014) Carboxymethylcellulose film for bacterial wound infection control and healing
506 CARBOHYD POLYM 112:367-375

507 Yu JR et al. (2019) Current and future perspectives on skin tissue engineering: Key features of biomedical
508 research, translational assessment, and clinical application ADV HEALTHC MATER 8:1801471

509 Zhang M, Zhao X (2020) Alginate hydrogel dressings for advanced wound management INT J BIOL
510 MACROMOL

511

512

513

514

515

516

517

518 **Figure captions**

519 **Fig. 1** Full thickness wound healing model in diabetic Wistar rats

520 **Fig. 2** Scanning electron microscopy images of (a) Calcium alginate/CMC films, (b) PVA fibers loaded with 5%
521 Propionyl-L-carnitine

522 **Fig. 3** The swelling percentages of Calcium alginate/CMC films over a period of 72 h

523 **Fig. 4** Cumulative release profile of Propionyl-L-carnitine from PVA nanofibers

524 **Fig. 5** Histogram comparing the blood compatibility of the experimental samples. Values represent the mean \pm SD, n
525 = 4, *P<0.05, **P <0.01 and ***P< 0.005

526 **Fig. 6** Histogram comparing the viability of L929 cells on (a) Calcium alginate/CMC films and (b) on PVA fibers at
527 1 day, 3 days, and 7 days after cell seeding. Values represent the mean \pm SD, n = 3, *P<0.05, **P <0.01 and
528 ***P< 0.005

529 **Fig.7** Microbial barrier property of the bilayer wound dressing after 3 and 7 days of incubation measured by
530 Spectrophotometer at 600 nm

531 **Fig. 8** Histogram comparing (a) percentage of wound closure at 7 days and 14 days post-wounding of different groups,
532 (b) epithelial thickness of different experimental groups, and (c) the percentage of collagen deposition in different
533 groups. Values represent the mean \pm SD, n = 5, *P<0.05, **P <0.01 and ***P< 0.005

534 **Fig. 9** Hematoxylin and Eosin (H&E) and Masson's trichrome (MT) stained microscopic sections (200x
535 magnification) of wound tissues treated with different dressings 14 days' post-treatment. Thick arrows: epidermal
536 thickness, thin arrows: recruitment of inflammatory cells, arrowheads: skin appendages, red arrows:
537 neovascularization

538

539

Figures



Figure 1

Full thickness wound healing model in diabetic Wistar rats

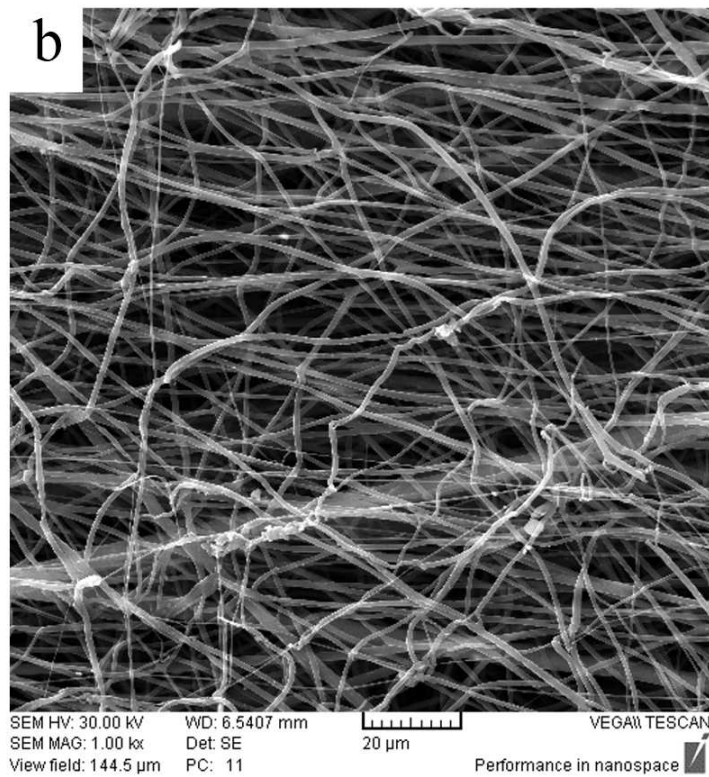
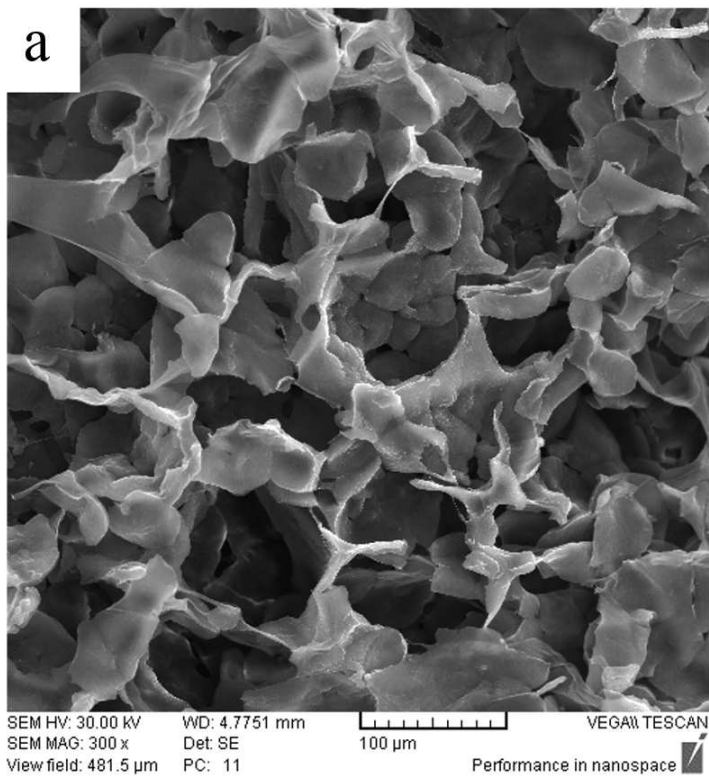


Figure 2

Scanning electron microscopy images of (a) Calcium alginate/CMC films, (b) PVA fibers loaded with 5% Propionyl-L-carnitine

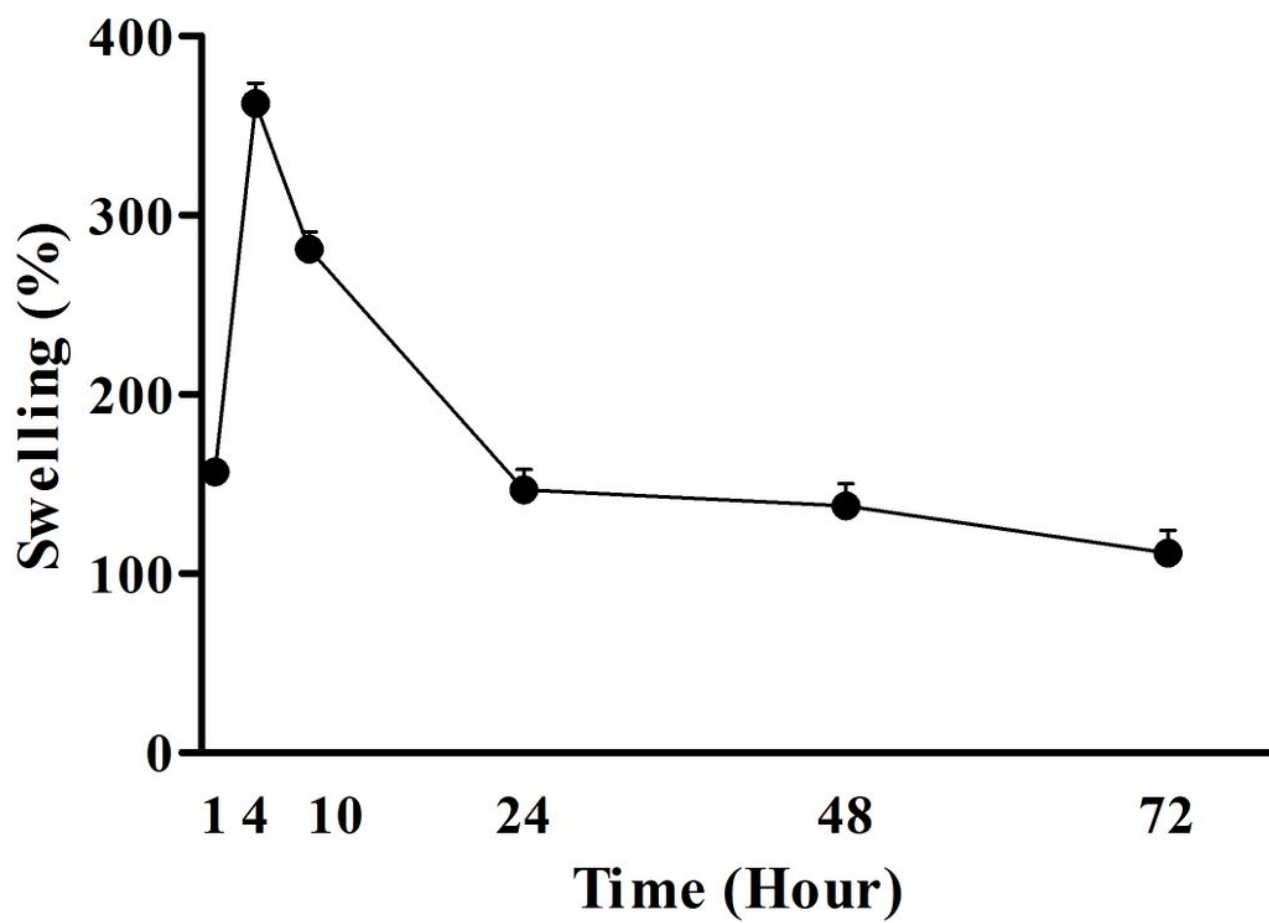


Figure 3

The swelling percentages of Calcium alginate/CMC films over a period of 72 h

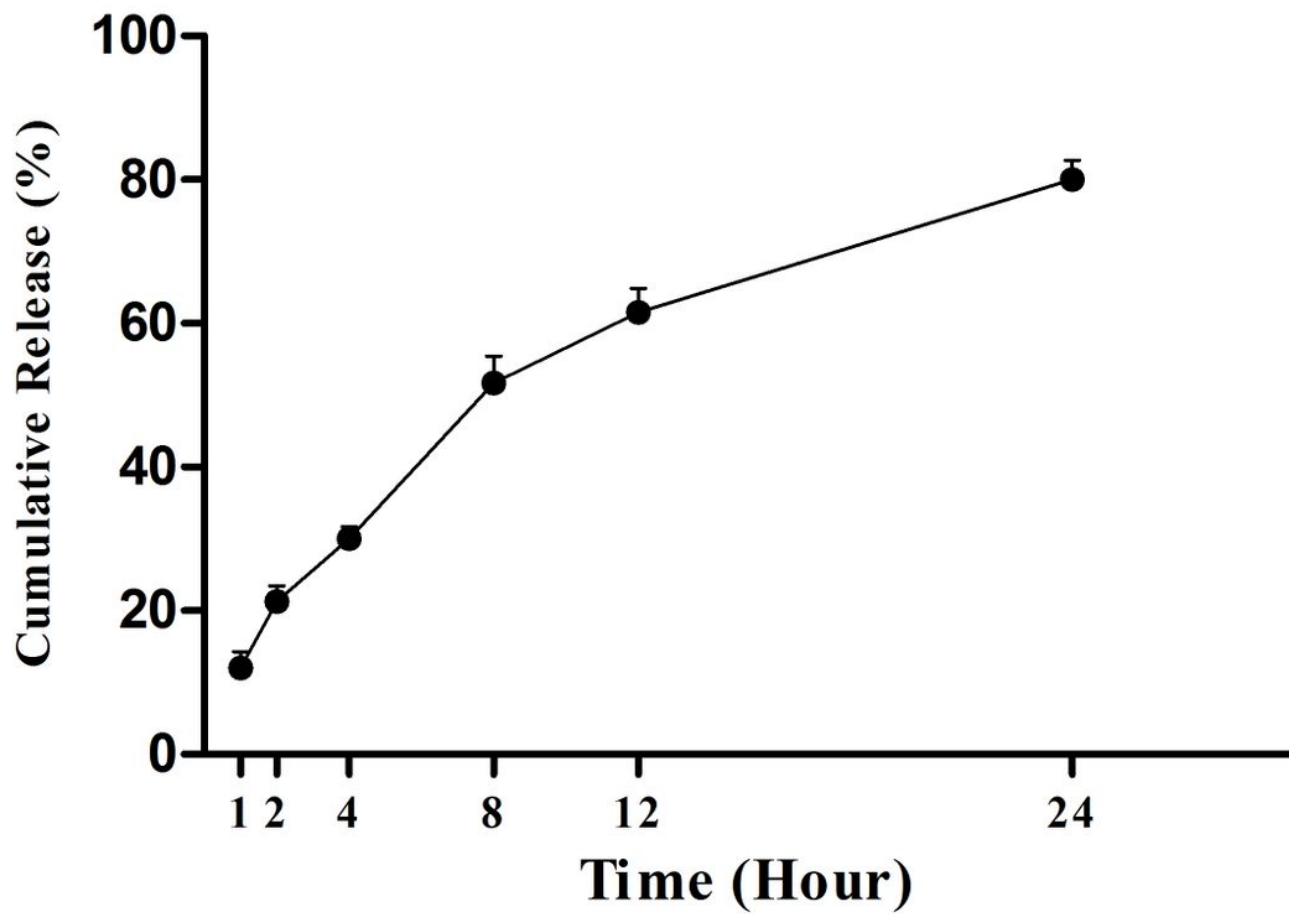


Figure 4

Cumulative release profile of Propionyl-L-carnitine from PVA nanofibers

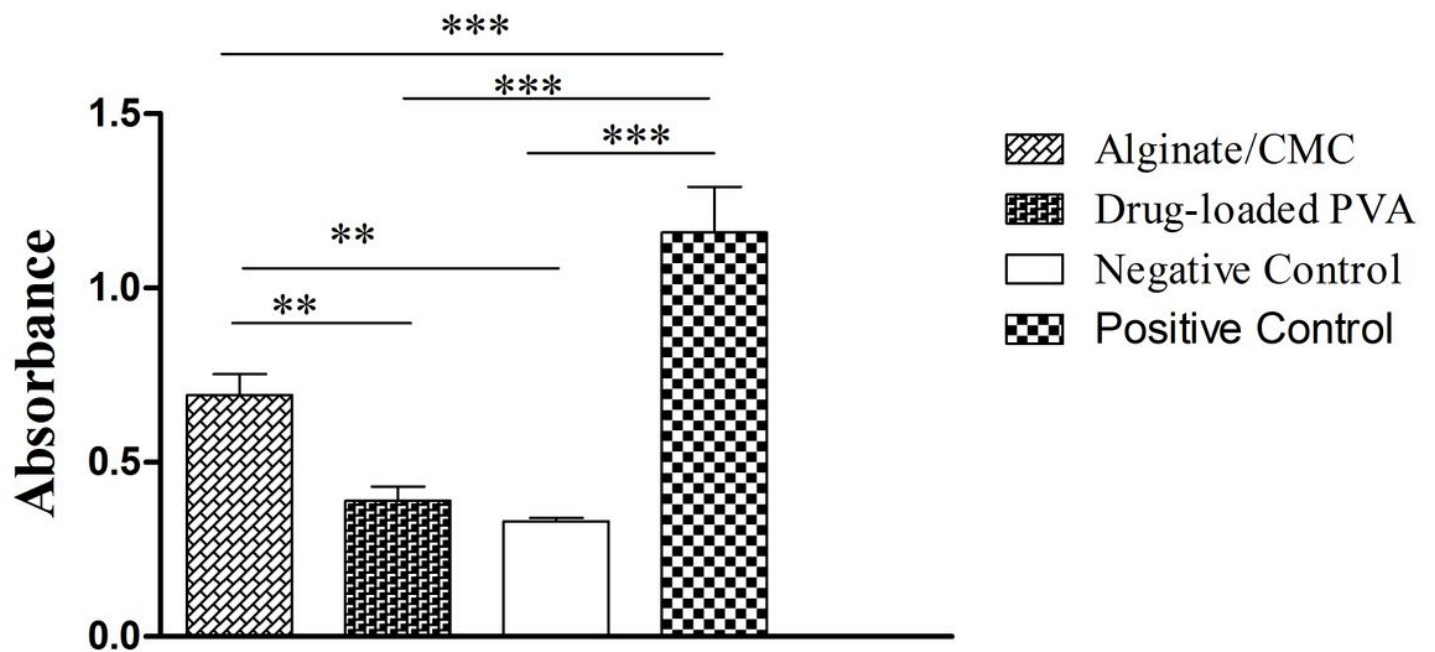


Figure 5

Histogram comparing the blood compatibility of the experimental samples. Values represent the mean \pm SD, n = 4, *P<0.05, **P <0.01 and ***P< 0.005

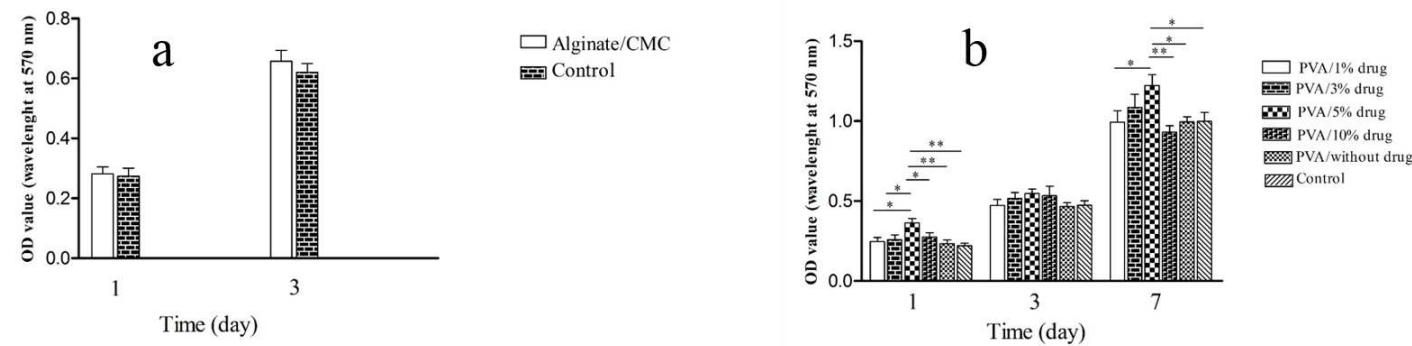


Figure 6

Histogram comparing the viability of L929 cells on (a) Calcium alginate/CMC films and (b) on PVA fibers at 1 day, 3 days, and 7 days after cell seeding. Values represent the mean \pm SD, n = 3, *P<0.05, **P <0.01 and ***P< 0.005

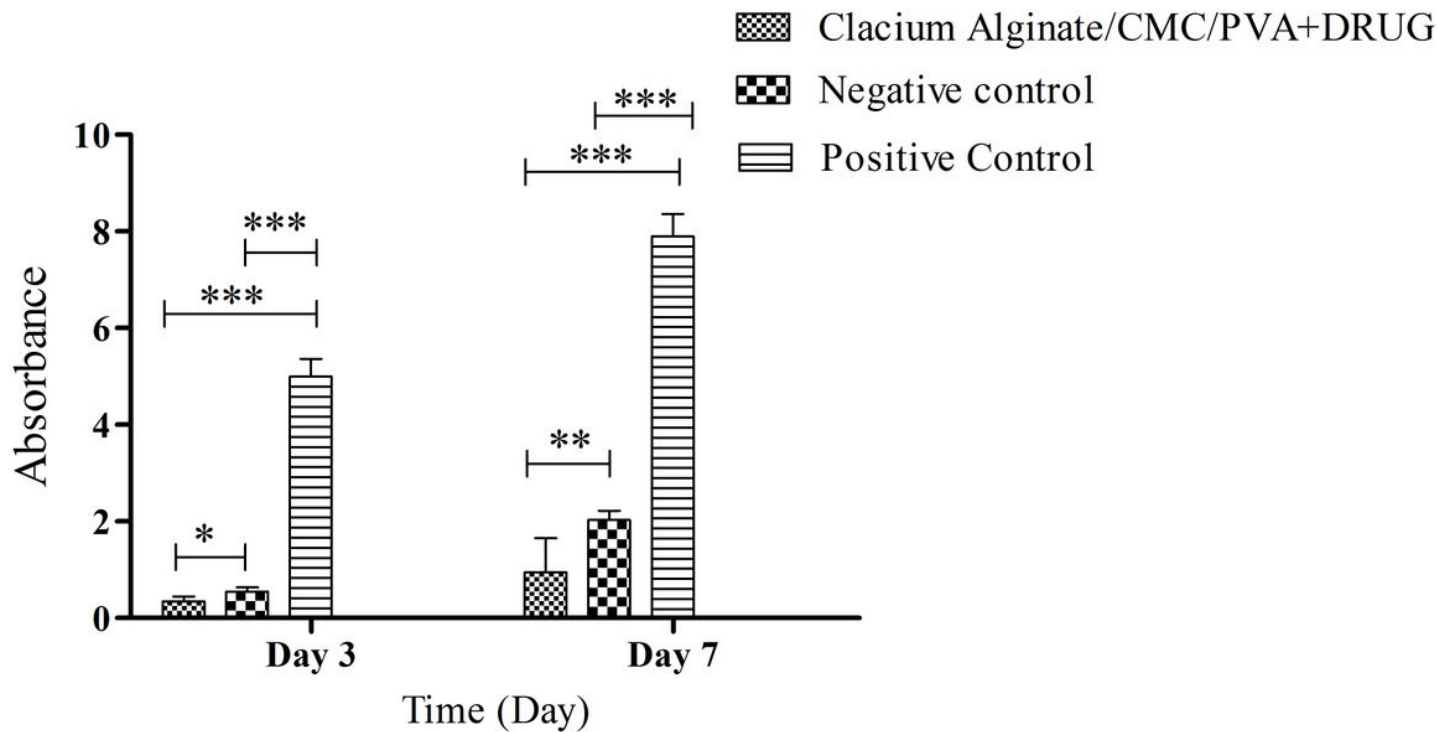


Figure 7

Microbial barrier property of the bilayer wound dressing after 3 and 7 days of incubation measured by Spectrophotometer at 600 nm

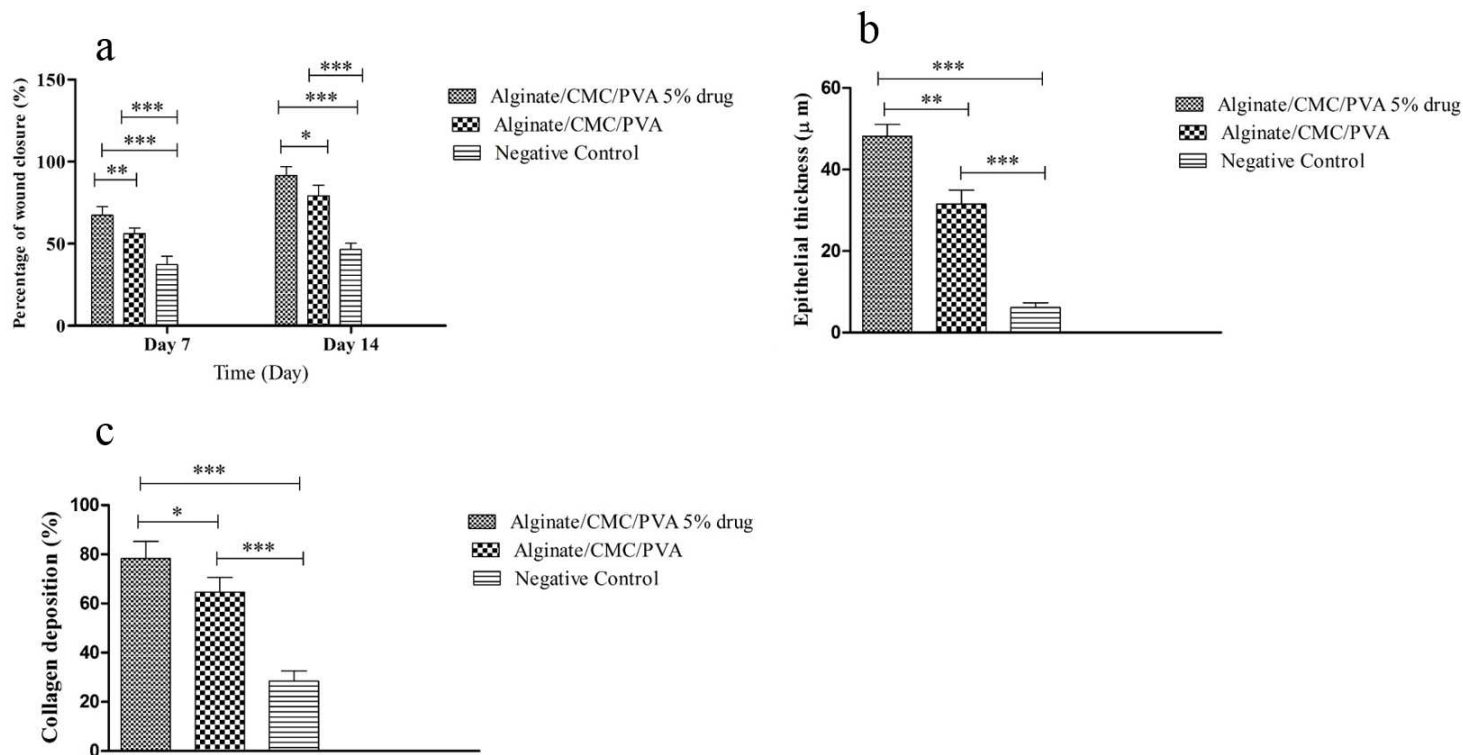


Figure 8

Histogram comparing (a) percentage of wound closure at 7 days and 14 days post-wounding of different groups, (b) epithelial thickness of different experimental groups, and (c) the percentage of collagen deposition in different groups. Values represent the mean \pm SD, n = 5, *P<0.05, **P <0.01 and ***P< 0.005

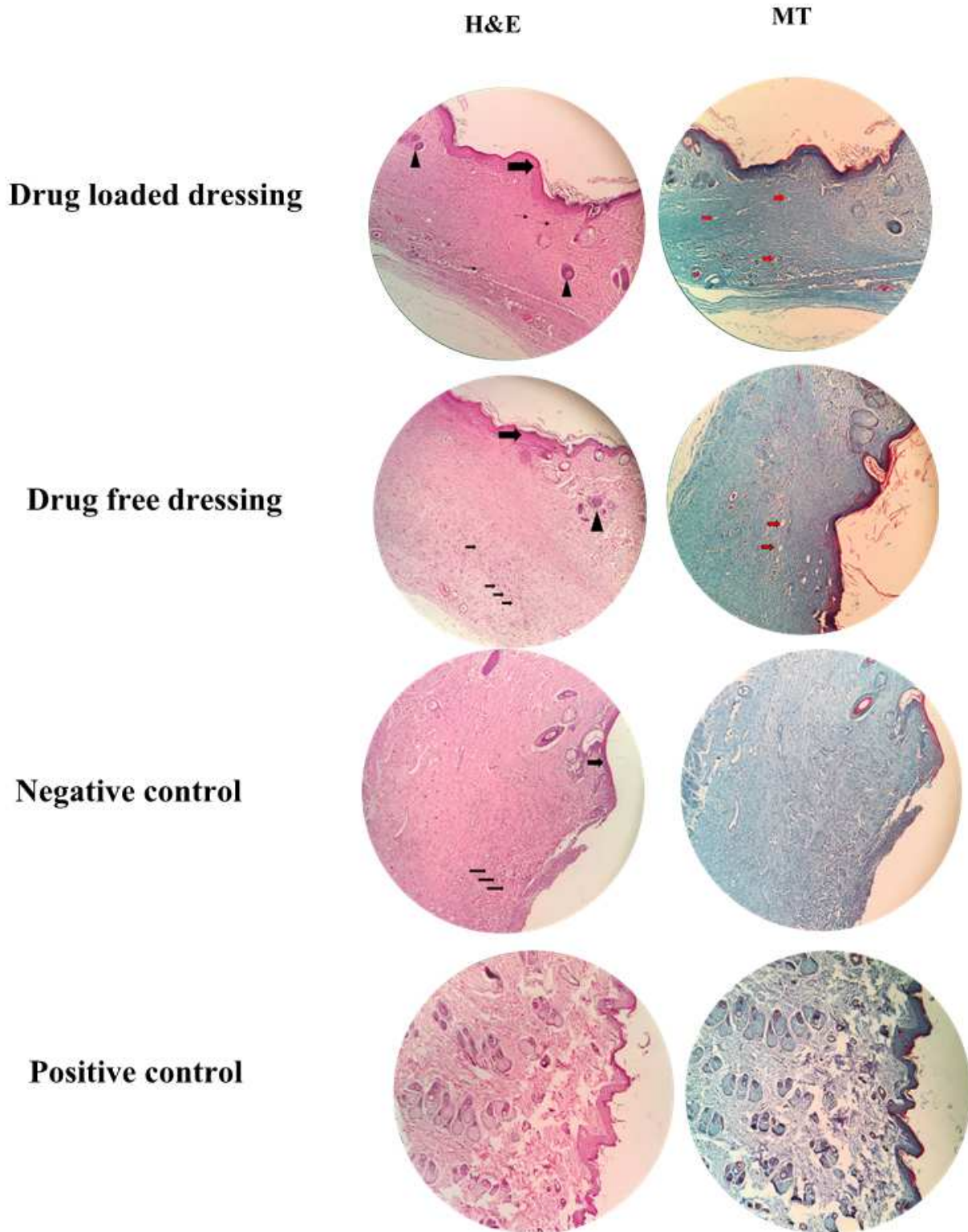


Figure 9

Hematoxylin and Eosin (H&E) and Masson's trichrome (MT) stained microscopic sections (200x magnification) of wound tissues treated with different dressings 14 days' post-treatment. Thick arrows: epidermal thickness, thin arrows: recruitment of inflammatory cells, arrowheads: skin appendages, red arrows: neovascularization